# A FAST INVERSE SOLVER FOR THE FILTRATION FUNCTION FOR FLOW OF WATER WITH PARTICLES IN POROUS MEDIA

A.C. ALVAREZ, P. G. BEDRIKOVETSKY, G. HIME, D. MARCHESIN, AND J. R. RODRIGUEZ

ABSTRACT. Models for deep bed filtration in the injection of sea water with solid inclusions depend on an empirical filtration function that represents the rate of particle retention. This function must be calculated indirectly from experimental measurements of other quantities. The practical petroleum engineering purpose is to predict injectivity loss in the porous rock around wells. In this work, we determine the filtration function from the effluent particle concentration history measured in laboratory tests knowing the inlet particle concentration.

The recovery procedure is based in solving a functional equation derived from the model equations. Well-posedness of the numerical procedure is discussed. Numerical results are shown.

*Inverse problem, Formation damage, Deep bed filtration, Iterative functional equation, System of convection-reaction equations*

## 1. INTRODUCTION

Most of the oil in the world is produced by injecting water in some wells and recovering oil in other wells. The recovered oil comes with reservoir water, which contains oil droplets and solid particles. The produced water must be separated from the oil and discarded taking environmental precautions. In off-shore fields, produced water and sea water are injected. However, the injection of poor quality water in a well curtails its injectivity because the particles suspended in the fluid are trapped while passing through the porous rock. This is due to particle retention in the pores, or *deep bed filtration*. In this paper we study the deep bed filtration during injection of water containing solid particles, which is essential to predict the loss of injectivity in wells.

Many laboratory studies were carried out to understand the filtration process ([7], [8]). Our work utilizes the model for deep bed filtration, developed in [2] based on the fundamental work of Hertzig et al. [8], which consists of equations expressing the particle mass conservation and the particle retention process ([3], [8], [13]). They form a quasi-linear hyperbolic system of equations containing the empirical *filtration function* $\lambda(\sigma)$, which represents the kinetics of particle retention.

Methods for determining the filtration function from the effluent concentration history at the core outlet $c_e(T)$ were presented in [14] and [17], for constant filtration $\lambda$. A recovery method for the general case was presented in [4] and [2], under the assumption that the injected particle concentration is constant.

In this work a method for obtaining the filtration function is studied relaxing the assumption made in [4] of constant injected particle concentration. The inverse problem consists of determining $\lambda(\sigma)$ from the outlet and inlet particle concentration histories $c_e(T)$ and $c_i(T)$. The recovery method reduces to solving a functional equation, which is derived from an invariant along the characteristic lines. The effluent concentration history $c_e(T)$ is measured in laboratory experiments. Because of cake formation, $c_i(T)$ is smaller than the particle

1

concentration in the fluid used in the injection experiment. This cake consists of particles that do not succeed in penetrating the wall where fluid is injected.

The paper is organized as follows. In Section 2 we present the deep bed filtration model as a quasi-linear system of hyperbolic equations. Existence, uniqueness and continuous dependence on the initial and boundary condition are discussed. In Section 3, the inverse problem solved in this work is presented, transformed into a functional equation. We prove that this equation has a unique solution that depends on the given data in a weakly continuous way. In Section 4, numerical stability is discussed. In Section 5, the numerical results are shown. Our results are summarized in Section 6.

## 2. Global solution for the direct problem in one dimension

We assume that water is incompressible, that the mass density of solid particles in suspended and entrapped states are both equal to the water density and that it is injected at constant volumetric rate. Neglecting diffusive effects, the mass conservation equation ([2], [7]) for the particles can be written in nondimensional form as:

$$\frac{\partial}{\partial T}(c + \sigma) + \frac{\partial c}{\partial X} = 0. \tag{2.1}$$

Here $c(X, T)$ and $\sigma(X, T)$ are the concentrations of the particles suspended in the water and entrapped by the rock, respectively, at position $X$ and time $T$. The time $T$ is in a nondimensional unit called pore volume or PV. The quantities $c$ and $\sigma$ have values between 0 and 1, but usually $c \cong 10^{-4}$; the independent variables satisfy $0 \leq X \leq 1$ and $T \geq 0$. The model ([2], [8]) requires a law for particle deposition rate. In non dimensional form this law is:

$$\frac{\partial \sigma}{\partial T} = \lambda(\sigma)c. \tag{2.2}$$

The right hand side of Eq. (2.2) means that the retention probability is proportional to the available concentration of suspended particles. This concentration is in turn proportional to $c$ and to the flow velocity that was scaled out of Eqs. (2.1)-(2.2) in the nondimensionalization process.

Physically, (2.2) cannot be valid for large $c$ or $\sigma$. In particular, Eq. (2.2) cannot take into account release of deposited particles. The positive $\lambda(\sigma)$ is an empirical coefficient known as the *filtration function*, which cannot be measured directly.

We will see in Section 2.3 that (2.1)–(2.2) has two families of characteristic lines; one family has the form $T - X = $ constant, the other $X = $ constant.

2.1. **Boundary and initial conditions.** We assume that the solid particle concentration entering into the porous medium is given, i.e.,

$$X = 0: \quad c(0, T) = c_i(T) > 0, \quad T > 0. \tag{2.3}$$

Also, we assume that the experimental injected concentration $c_i$ is a positive continuously differentiable function for $T > 0$.

As initial data at $T = 0$, we assume that the rock contains water with no particles:

$$\sigma(X, 0) = 0 \quad \text{and} \quad c(X, 0) = 0. \tag{2.4}$$

Along the line $X = 0$ we obtain from Eq. (2.2) and (2.3):

$$\frac{d\sigma(0, T)}{dT} = \lambda(\sigma(0, T))c_i(T), \quad \text{and} \quad \sigma(0, 0) = 0. \tag{2.5}$$

Integrating Eq. (2.5) provides $\sigma(0, T)$, which is always positive and increasing.

## 2.2. The invariant along the characteristics.

Except at initial times, it turns out that $c$ is much smaller than $\sigma$. Because of this fact, Herzig et al. [8] proposed a simplified model comprising (2.2) and the following modified version of (2.1), where $\partial c/\partial T$ in (2.1) was neglected relative to $\partial \sigma/\partial T$:

$$\frac{\partial \sigma}{\partial T} + \frac{\partial c}{\partial X} = 0. \tag{2.6}$$

For the model (2.2) and (2.6), under the assumption (2.4a), Herzig et al. in [8] proved the following relationship between the deposited and suspended particle concentrations along characteristic lines:

$$\frac{\sigma(X, T)}{c(X, T)} = \frac{\sigma(0, T - X)}{c(0, T - X)}, \tag{2.7}$$

which is valid for $T > X$, $0 \leq X \leq 1$. However, the same relationship was stated in [4] for the full model (2.1), (2.2) based on an incomplete derivation. Because (2.7) is the basis of the method for determining $\lambda(\sigma)$, here we provide a proof. The reader interested only in the inverse problem may skip the rest of Section 2.

We make the following positivity assumption:

**Assumption 2.1.** The filtration function is a positive $C^1$ function of $\sigma$ in $0 \leq \sigma < 1$, such that $\lambda(\sigma) > 0$ for $0 \leq \sigma < 1$.

This assumption is somewhat stringent in practical applications because $\lambda(\sigma)$ may vanish for colloidal suspensions. From Assumption 2.1, we can define the first integral $\Psi$ of $1/\lambda$, i.e., we can choose $\Psi$ so that $\Psi(0) = 0$ as follows:

$$\Psi(\sigma) = \int_0^\sigma \frac{d\eta}{\lambda(\eta)}. \tag{2.8}$$

Let us introduce the notation

$$m = \int_0^1 \frac{d\eta}{\lambda(\eta)}, \tag{2.9}$$

Depending on the behavior of $\lambda(\sigma)$ near 1, the range of $\Psi : [0, 1) \to [0, m)$ is either a finite or infinite interval.

Let us consider a solution of (2.1)–(2.4); we can expect that it is $C^1$ except at the characteristic line $X = T$, because there is a mismatch between the initial and boundary data for $c$ at $(0, 0)$. We will focus our attention on the trapezoid $\{(X, T) : 0 \leq X \leq 1, \ T \geq X \geq 0\}$, see Fig. 2.1, and make the following assumption, which will be justified in Theorem 1:

$$\sigma(X, T) = 0 \quad \text{for} \quad T = X, \text{ just above the trapezoid lower edge.} \tag{2.10}$$

**Lemma 2.2.** *Assume that there exists a $C^1$ solution of* (2.1)–(2.3) *in the trapezoid, satisfying* (2.10)*. Then $\sigma/c$ is constant along characteristic lines with slope 1.*

Proof: Differentiating Eq. (2.8) and using Eq. (2.2) we obtain

$$\frac{\partial \Psi(\sigma)}{\partial T} = c \quad \text{for} \quad \sigma \quad \text{in} \quad [0, 1). \tag{2.11}$$

Since $\Psi$ is $C^2$ the derivatives of (2.11) are

$$\frac{\partial c}{\partial T} = \frac{\partial^2 \Psi(\sigma)}{\partial T^2}, \qquad \frac{\partial c}{\partial X} = \frac{\partial^2 \Psi(\sigma)}{\partial T \partial X} \tag{2.12}$$

are well defined for $X \neq T$. Substituting the expressions (2.11) and (2.12) in (2.1) we have

$$\frac{\partial^2 \Psi(\sigma)}{\partial T^2} + \frac{\partial^2 \Psi(\sigma)}{\partial T \partial X} = -\frac{\partial \sigma}{\partial T} \quad \text{or} \quad -\frac{\partial}{\partial T}\left(\frac{d\Psi(\sigma)}{dX}\right) = -\frac{\partial \sigma}{\partial T}, \tag{2.13}$$

which is well-defined for $X \neq T$. In (2.13b) $\frac{d}{dX}$ is the differentiation along characteristic lines $T - X = constant$, i.e. $\frac{d}{dX} = \frac{\partial}{\partial X} + \frac{\partial}{\partial T}$, see Fig. 2.1.

Now, we consider (2.13) in the infinite trapezoid $\{(X, T) : 0 \leq X \leq 1, \ T \geq X \geq 0\}$. Integrating (2.13b) in $T$ along a vertical line from the point $(X, X)$ on the lower edge of the trapezoid to a fixed $(X, T)$ we obtain

$$\left.\frac{d\Psi(\sigma)}{dX}\right|_{(X,T)} - \left.\frac{d\Psi(\sigma)}{dX}\right|_{(X,X)} = \sigma\Big|_{(X,T)} - \sigma\Big|_{(X,X)}. \tag{2.14}$$

Using (2.8) and (2.10) we see that $\sigma|_{T=X} = 0$ and $\left.\frac{d\Psi(\sigma)}{dX}\right|_{T=X} = 0$; using these expressions in (2.14) we obtain (2.15a). Using Eqs. (2.1) and (2.2) we obtain (2.15b)

$$\frac{d\sigma}{dX} = -\lambda(\sigma)\sigma \quad \text{and} \quad \frac{dc}{dX} = -\lambda(\sigma)c. \tag{2.15}$$

In summary, we have proved that if (2.1)–(2.2) has a $C^1$ solution in the trapezoid satisfying (2.5), (2.10), then this solution must satisfy (2.15) in the trapezoid. From Eqs. (2.15a) and (2.15b), we obtain along characteristic lines

$$\frac{d\sigma}{dc} = \frac{\sigma}{c}. \tag{2.16}$$

Integrating Eq. (2.16) along characteristic lines with slope 1, we obtain that $\sigma/c$ is invariant along such lines, hence (2.7) holds. $\square$

### 2.3. **Well posedness of the direct problem.** The system (2.1)–(2.2) can be rewritten as

$$\frac{\partial}{\partial T}\begin{pmatrix} c \\ \sigma \end{pmatrix} + \begin{pmatrix} 1 & 0 \\ 0 & 0 \end{pmatrix}\frac{\partial}{\partial X}\begin{pmatrix} c \\ \sigma \end{pmatrix} = \begin{pmatrix} -\lambda(\sigma) & 0 \\ \lambda(\sigma) & 0 \end{pmatrix}\begin{pmatrix} c \\ \sigma \end{pmatrix}, \tag{2.17}$$

which is a quasi-linear hyperbolic system. This system has two characteristic directions, which are $(dX, dT)^T = (1, 1)^T$ (with speed 1) and $(dX, dT)^T = (0, 1)^T$ (with speed 0), see Fig 2.1.

**Theorem 2.3.** *There exists a unique, well-posed weak solution of* (2.1)–(2.4) *in the infinite rectangle for $C^1$ boundary data $c_i(T)$, $T > 0$. This solution vanishes in the triangle with vertices $(0, 0)$, $(0, 1)$, $(1, 1)$ in Fig. 2.1; it is $C^1$ in the trapezoid above the triangle, where it is given by the unique solution of family of the ODE's* (2.5), (2.15).

Proof: We consider the system (2.17) in the triangle $\{(X, T) : 0 \leq T \leq X \leq 1\}$ with initial data (2.4). It follows from the method of characteristics described in Section 5, Chapter 2, [9] and Section 2, Chapter 5, [6] that the only solution in the triangle vanishes identically. This is illustrated by the two characteristic lines reaching the point $(X, T)$ in the triangle shown in Fig. 2.1: since $\sigma$ and $c$ vanish at the feet of characteristics, they vanish at $(X, T)$.

Let us consider bounded weak solutions of (2.1), (2.2) defined near the line $X = T$ (see Fig 2.1), in the sense of [9]. Integrating (2.2) along segments with fixed $X$ for $0 < X \leq 1$
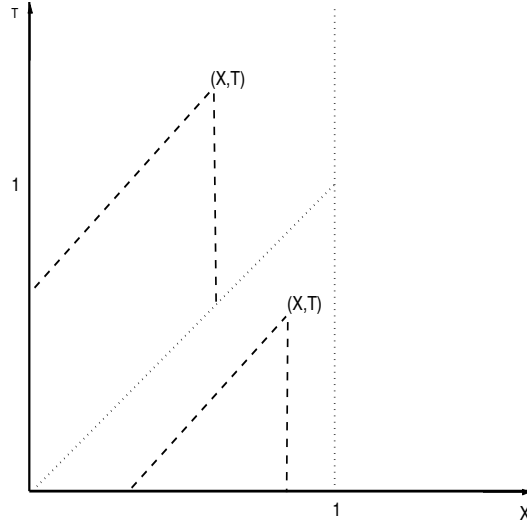
FIGURE 2.1. Characteristic lines; triangle (lower) and trapezoid (upper).

from $T - \epsilon$ to $T + \epsilon$, where $\epsilon$ is positive and small we see that

$$\lim_{\epsilon \to 0} \{\sigma(X, T + \epsilon) - \sigma(X, T - \epsilon)\} = 0.$$

Thus (2.10) holds. Performing the same integration on (2.1) yields no new information, i.e. $c(X, T)$ may be nonzero on $T = X$, just above the trapezoid lower edge from $(0, 0)$ to $(1, 1)$; in other words, there may be a shock along $T = X$.

Now, let us focus on the infinite trapezoid $\{(X, T) : 0 \leq X \leq 1, \ T \geq X \geq 0\}$. Consider the unique $C^1$ solution $\sigma(X, T)$, $c(X, T)$ of (2.5) and (2.15) in the trapezoid. Notice that (2.14), (2.13), (2.12) and (2.11) hold, therefore (2.1)–(2.2) hold and this is the only solution of system (2.1)–(2.4) in the trapezoid. This solution is $C^1$ in the trapezoid.

In summary, the system (2.1)–(2.4) has a unique solution on the infinite rectangle. This solution has a jump in $c$ along the front $X = T$. This is the unique global weak solution of (2.1)–(2.2) under proper initial and boundary conditions and the assumption (2.1) on the filtration function $\lambda(\sigma)$. $\square$

**Remark 2.4.** Since along the front trajectory $X = T$ the deposited concentration is zero, i.e., (2.10) holds, we obtain the following ordinary differential equation for $c(X, X)$ along this line in the trapezoid:

$$\frac{dc(X, X)}{dX} = -\lambda(0)c(X, X). \tag{2.18}$$

Integrating (2.18) and using (2.3) at $T = 0$, we obtain

$$c(X, X) = c_i(0) \exp(-\lambda(0)X). \tag{2.19}$$

Since $c_i(0) > 0$, from (2.19) we obtain that $c(X, X)$ is positive for $X > 0$ in the trapezoid and 0 below; so there is indeed a shock along the characteristic $X = T$, as shown in Figure (2.2a).

**Remark 2.5.** The system of equations (2.5), (2.15) is convenient for using standard ODE procedures to solve numerically the PDE.

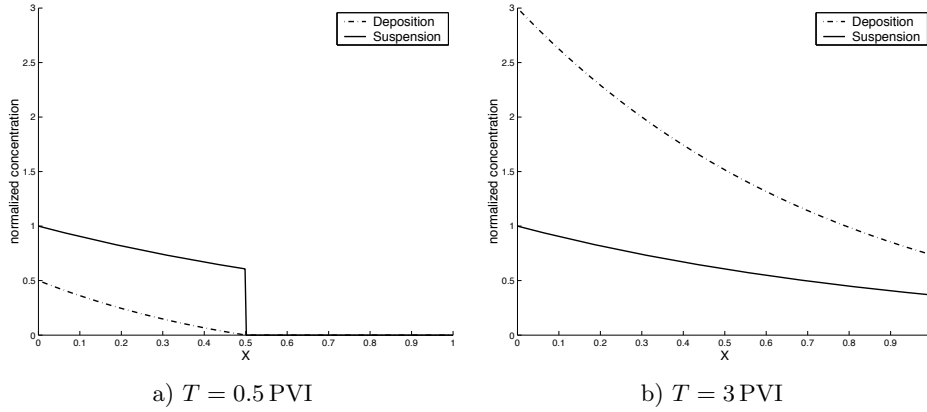a) $T = 0.5\,\mathrm{PVI}$                    b) $T = 3\,\mathrm{PVI}$

FIGURE 2.2. Typical normalized suspended and deposited particle concentrations before and after breakthrough: notice the discontinuity at $T = X$ on the left figure.

**Remark 2.6.** If we take the experimental data function $c_i(T)$ to be $C^2$ instead of $C^1$, then the solution $\sigma$, $c$ of the system (2.1)–(2.4) is $C^2$ in the trapezoid. In particular, the predicted effluent concentration $c(1, T)$ is a $C^2$ function for $T > 1$.

## 3. THE RECOVERY METHOD

Here we describe the recovery method for obtaining the filtration function in (2.17) from the injected and effluent concentration of particles. See also [1], [2], [4] [10], and [11]. An inverse problem for a system similar to (2.17) was studied in [5].

3.1. **Derivation of the functional equation.** Here we generalize [2] and [4], where only the case of constant injected concentration $c_i(T) = c_{io}$ was considered. It is useful to introduce the variable $z \geq 0$ and the notation

$$c_i(z) \equiv c(0, z) > 0, \quad c_e(z) \equiv c(1, z + 1) > 0, \quad \sigma_i(z) = \sigma(0, z), \quad \sigma_e(z) = \sigma(1, z + 1). \quad (3.1)$$

We assume here that the experimental data $c_i$, $c_e$ are $C^2$ functions for $0 \leq z < \infty$.

We will also need the $C^3$ functions on $0 \leq z < \infty$

$$\tau = C_i(z) \equiv \int_0^z c_i(s)ds, \quad C_e(z) \equiv \int_0^z c_e(s)ds. \quad (3.2)$$

From (3.1a) it follows that $C_i$ in (3.2a) is monotone increasing and $C_i(0) = 0$. Thus, from the implicit function theorem the inverse function $C_i^{(-1)}(\tau)$ of $C_i$ in (3.2a) and it is $C^3$. Moreover, this function is monotone increasing. We have

$$z = C_i^{(-1)}(\tau) \quad \text{or} \quad \frac{dz}{d\tau} = \frac{1}{c_i(z)} \quad \text{with} \quad z(0) = 0.$$

Because of Assumption 2.1, the definition (2.8) and $\Psi'(\sigma) = 1/\lambda(\sigma) > 0$, there exists the function $g : [0, m) \to [0, 1)$

$$\sigma = g(\psi), \quad \text{inverse of the function} \quad \psi = \Psi(\sigma); \quad (3.3)$$

notice that $g(0) = 0$. Relationships between the deposited and suspended particle concentrations at the inlet and outlet points $X = 0$ and $X = 1$ can be obtained as follows. We

integrate Eq. (2.11) in $z$, use (3.2) and $\sigma_i(0) = \sigma(0,0) = 0$, $\sigma_e(0) = \sigma(1,1) = 0$, i.e.,

$$\Psi(\sigma_i(z)) = C_i(z), \quad \Psi(\sigma_e(z)) = C_e(z). \tag{3.4}$$

Now, from (3.3) and (3.4) we obtain

$$\sigma_i(z) = g(C_i(z)), \quad \sigma_e(z) = g(C_e(z)) \quad \text{for} \quad z \geq 0. \tag{3.5}$$

Replacing $X$ by 1 and $T$ by $T+1$ in (2.7) and using (3.1) with $z = T$ we obtain:

$$\frac{\sigma(1, T+1)}{c(1, T+1)} = \frac{\sigma(0, T)}{c(0, T)} \quad \text{or} \quad \frac{\sigma_e(z)}{c_e(z)} = \frac{\sigma_i(z)}{c_i(z)}. \tag{3.6}$$

Substituting the expressions (3.5) into Eq. (3.6$b$), we obtain the following functional equation for the function $\sigma = g(\psi)$:

$$g(C_e(z)) = \frac{c_e(z)}{c_i(z)} g(C_i(z)) \quad \text{or} \quad g(C_e(z)) = \frac{C'_e(z)}{C'_i(z)} g(C_i(z)) \quad \text{for} \quad z \geq 0. \tag{3.7}$$

Finally, using the definition of $\tau$ in (3.2) and denoting

$$D(\tau) \equiv C_e(C_i^{(-1)}(\tau)) \quad \text{and} \quad \theta(\tau) \equiv \frac{c_e(C_i^{(-1)}(\tau))}{c_i(C_i^{(-1)}(\tau))}, \tag{3.8}$$

equation (3.7) can be rewritten as

$$g(D(\tau)) = \theta(\tau)g(\tau) \quad \text{for} \quad \tau \geq 0. \tag{3.9}$$

Here $D$ and $\theta$ are known, so this is a functional equation for $g$ that needs to be solved.

For constant injected concentration $c_i(z) = c_{io}$, (3.9) reduces to Julia's equation, which is studied in [11]:

$$g(D(\tau)) = D'(\tau)g(\tau) \quad \text{for} \quad \tau \geq 0. \tag{3.10}$$

The recovery method outlined in [4] is based on the functional equation (3.10); a formula for the solution of (3.10) is obtained by means of an iterative procedure. In the next section an analogous formula for the solution $g(\tau)$ of (3.9) is obtained for non-constant injected concentration $c_i(T)$.

From the definitions of $g$ in (3.3) and $\Psi$ in (2.8) we obtain

$$\lambda(\sigma) = g'(\sigma). \tag{3.11}$$

Thus, once the function $\sigma = g(\Psi)$ has been found by means of equation (3.9), we determine the filtration function $\lambda(\sigma)$ using (3.11).

**Remark 3.1.** We will see in the next section that the solution of (3.9) is proportional to $g'(0)$. Notice from (3.11) that $g'(0) = \lambda(0)$. This value is determined from (2.19) as follows:

$$g'(0) = \lambda(0) = -\log(c_e(0)/c_i(0)). \tag{3.12}$$

3.2. **Solution of the functional equation.** In this section the functional equation (3.9) is solved. We assume that the data $c_i(T)$, $c_e(T)$ are $C^2$, providing sufficient smoothness for the existence of a unique $C^2$ solution. Sufficient conditions for the existence and uniqueness of the solution of (3.9) are given in [11].

In practice, the values of the injected and effluent particle concentration are measured up to the final time $T_f$. So, we solve the equation (3.9) for $\tau$ in $[0, r]$, where $r = C_i(T_f)$.

**Remark 3.2.** Let $D : [0, r] \rightarrow [0, r)$ be a continuous monotone increasing function, such that $D(0) = 0$ and $D(\tau) < \tau$ in $(0, r]$. Let $\tau_0$ be any point in $(0, r]$. Consider the nonnegative sequence in $[0, r]$ given by $\tau_{n+1} = D(\tau_n)$, $n = 0, 1, 2, \ldots$. Then this sequence is monotone decreasing and it converges to 0 (see [1] or [10] for a proof).

Let us consider the Banach space with norm $||g|| = \sup_{[0,r]}\{|g(x)|\} + \sup_{[0,r]}\{|g'(x)|\} + \sup_{[0,r]}\{|g''(x)|\}$:

$$G_0 = \{C^2[0, r] \quad \text{such that} \quad g(0) = 0\}.$$

**Theorem 3.3.** *Let* $D : [0, r] \rightarrow [0, r)$ *be a* $C^2$ *monotone increasing function, such that* $D(0) = 0$ *and* $D(\tau) < \tau$ *in* $(0, r]$. *Let* $\theta : [0, r] \rightarrow (0, 1)$ *be a* $C^2$ *function, satisfying* $0 < \theta(\tau) < 1$ *and* $[D'(0)]^2/\theta(0) < 1$. *Furthermore, consider the functional equation (3.9) on* $G_0$, *i.e.*

$$g\big(D(\tau)\big) = \theta(\tau)g(\tau) \quad for \quad \tau \quad in \quad (0, r). \tag{3.13}$$

*Then the functional equation (3.13) has a solution in* $G_0$, *which is uniquely defined by the value of* $g'(0)$.

**Proof:** The existence of a unique $C^2$ solution of the functional equation (3.13) is guaranteed by Theorem 3.4.2 in [11]. Now, an iterative formula for the solution of (3.13) is presented in Theorem 5.8 in [10], which depends on an arbitrary function. Here we determine the solution as follows.

Let us assume that given $D$ and $\theta$ as above there exists a $g$. We present an algorithm or formula for $g$. To compute $g(\tau_0)$ for any $0 < \tau_0 < r$, we define the two infinite sequences

$$\tau_1 = D(\tau_0), \quad \tau_2 = D(\tau_1), \quad \ldots \quad \tau_n = D(\tau_{n-1}),$$

$$q_1 = \theta(\tau_0), \quad q_2 = \theta(\tau_1)q_1, \quad \ldots \quad q_n = \theta(\tau_{n-1})q_{n-1},$$

or

$$\tau_n = D^n(\tau_0), \qquad q_n = \prod_{k=0}^{n-1} \theta(\tau_k).$$

From Remark 3.2, $\tau_n$ tends to zero monotonically. Notice that $\tau_1 = D(\tau_0)$ is continuous in $\tau_0$, and so is $\tau_n = D^n(\tau_0)$. Similarly, since $\theta$ is continuous, $q_n$ is a continuous function of $\tau_0$. The following lemma is proved in [10].

**Lemma 3.4.** $\lim\limits_{n\to\infty} q_n(\tau_0) = 0$ *uniformly for* $\tau_0 \in [0, r)$.

From the functional equation (3.13), it follows that

$$g(\tau_k) = g(D(\tau_{k-1})) = \theta(\tau_{k-1})g(\tau_{k-1}),$$

so by repeated use of the formula above for $k = n, n-1, \cdots, 1$ we obtain

$$g(\tau_n) = g(\tau_0) \prod_{k=0}^{n-1} \theta(\tau_k). \tag{3.14}$$

On the other hand, using the definition of derivative and $g(0) = 0$ we obtain

$$g'(0) = \lim_{n\to\infty} \frac{g(\tau_n) - g(0)}{\tau_n - 0} = \lim_{n\to\infty} \frac{g(\tau_n)}{\tau_n}. \tag{3.15}$$

Substituting (3.14) in (3.15), we see that

$$g'(0) = g(\tau_0) \lim_{n \to \infty} \frac{\prod_{k=0}^{n-1} \theta(\tau_k)}{\tau_n}. \tag{3.16}$$

Thus, we obtain the solution for the functional equation (3.13) for any $\tau_0 > 0$:

$$g(\tau_0) = g'(0) \lim_{n \to \infty} \frac{\tau_n}{\prod_{k=0}^{n-1} \theta(\tau_k)} \quad \text{or} \quad g(\tau_0) = g'(0) \lim_{n \to \infty} \frac{\tau_n}{q_n}. \tag{3.17}$$

The formula (3.17) can be rewritten as an infinite product, which is very useful for numerical calculations. Let us define

$$R_n = \frac{\tau_n}{\prod_{k=0}^{n-1} \theta(\tau_k)}, \quad \rho_n = \frac{D(\tau_n)}{\theta(\tau_n)\tau_n}. \tag{3.18}$$

Then

$$R_n = \frac{D(\tau_{n-1})\tau_{n-1}}{\theta(\tau_{n-1})\tau_{n-1} \prod_{k=0}^{n-2} \theta(\tau_k)} = \frac{D(\tau_{n-1})}{\theta(\tau_{n-1})\tau_{n-1}} R_{n-1} = \rho_{n-1} R_{n-1}, \tag{3.19}$$

so that

$$g(\tau_0) = g'(0) \prod_{n=0}^{\infty} \frac{D(\tau_n)}{\theta(\tau_n)\tau_n} \quad \text{or} \quad g(\tau_0) = g'(0) \prod_{n=0}^{\infty} \rho_n. \tag{3.20}$$

Eq. (3.20) is the basis of the algorithm for solving the functional equation.

**Remark 3.5.** Now it is possible to verify that the functional equation in (3.9) satisfies the assumptions of Theorem 3.3. To do so, we take into account the following facts. Applying Gronwall's inequality into (2.15b), it was proved in [1] that $c_e(\tau) < c_i(\tau)$ for $\tau \geq 0$; it follows that $0 < \theta(\tau) < 1$ for $\tau \geq 0$. Moreover, using (3.8) one verifies that $D'(0) = \theta(0)$, so the inequality $[D'(0)]^2/\theta(0) = \theta(0) < 1$ is satisfied.
Now, since $0 < \theta(\tau) < 1$ and $c_e(\tau) < 1$ for $\tau > 0$, we obtain that $D(\tau) < \tau$ for $\tau > 0$. Finally, $D(\tau)$ and $\theta(\tau)$ are $C^2$ functions because the functions $c_i$ and $c_e$ are $C^2$.

**Remark 3.6.** For Julia's equation the formula (3.20) reduces to

$$g(\tau_0) = g'(0) \prod_{n=0}^{\infty} \frac{D(\tau_n)}{D'(\tau_n)\tau_n}, \quad \text{with} \quad D(\tau) = C_e(\tau/c_{i0}). \tag{3.21}$$

**Remark 3.7.** Once the solution $g$ of the functional equation (3.9) is obtained, we can solve the direct problem (2.1)–(2.4) using the filtration function $\lambda(\sigma)$ determined by (3.11) and find $c(1, T)$. It is possible to verify, using the method described in Section 3 and Theorem 3.3, that the correspondent effluent concentration function $c(1, T)$ coincides with the input data $c_e(T)$ in (3.1b) used in the recovery procedure.

We have proved the following:

**Theorem 3.8.** *Given the $C^2$ functions $c_i(T)$, $c_e(T)$, there exists a unique $\lambda(\sigma)$, (which is $C^1$) such that the problem (2.1)–(2.4) has a solution satisfying $c(1, T) = c_e(T)$.*

**Remark 3.9.** More generally, it is possible to prove that given $C^m$ functions $c_i(T)$, $c_e(T)$, the filtration function $\lambda(\sigma)$ is $C^{m-1}$.

## 4. Stability

In summary, the method for obtaining the filtration function in Section 3 consists of the following sequence of calculations

$$\{c_i, c_e\} \to \{C_i, C_e\} \to \{D, \theta\} \to g \to \lambda,$$

where "$\to$" represents a procedure to obtain output functions from the previous data. To obtain stable numerical methods for calculating the approximate solution of the filtration function, we must study the well posedness of Eqs. (3.2), (2.8) and (3.9).

Clearly the functions $C_i$ and $C_e$ depend continuosly on $c_i$ and $c_e$ respectively. The functions $D$ and $\theta$ depend continuosly on $c_i$, $c_e$ as well. In [11] it was proved that the solution of the functional equation (3.9) depends continuously on the functions $D(\tau)$ and $\theta(\tau)$, so the solution $g$ depends continuously on the functions $c_i$ and $c_e$. Finally, the stability of the recovery method requires that the numerical differentiation of the solution $g$ of (3.9) is performed in a stable way. We have used cubic splines for numerical differentiation; however, better approximations such as smoothing splines perhaps would lead to less oscillating filtration functions ([15], [16]). Also, from the definition of $\Psi$ in (2.8), we can expect that serious numerical instabilities arise when the filtration function values are very small.

## 5. Numerical results

In this section the implementation of the numerical method for solving the functional equation is described, along with the experiments we performed over real measurement data, their results and brief discussion.

5.1. **Implementation.** We have implemented the product form presented in (3.21) (Julia's equation), assuming that $c_i(T)$ is a constant $c_{i0}$. The algorithm takes this constant and a time series $(T, c_e(T))$ as input. Data are filtered so that only the pairs with $T \geq 1$ for which $c_e(T) > 0$ are used. Ideally, the time value $T_0$ of the first of these pairs is 1, but not in practice: in the four cases we studied, it was in the range $[4.26, 7.75]$. To provide for the missing datum $c_e(1)$, and also to obtain a dense data set from the sparse points available, we have added arbitrarily the point $(T = 0, c_e(0) = 0)$ to the data series and then we used cubic spline interpolation to obtain a smooth, dense set with which includes the point $(1, c_e(1))$.

The time series is not necessarily evenly spaced. Over this time grid we compute the auxiliary quantity $D(\tau)$, using standard trapezoidal integration. Next we compute the cubic spline used to evaluate the function $D(\tau)$, stored as a discrete series, and its derivative. Since $D(\tau)$ is the integral of $c_e(T)$, we know its first derivative at the end points, and use it when computing the spline coefficients.

We now proceed to the computation of $g(\tau)$ as in (3.21). We create an evenly spaced mesh for $\Psi$ in (2.8) covering the interval $[0, T_f]$, the whole span for which data is available. Over this mesh, we compute the values of $g$ iteratively as a truncated infinite product. The criterium for trucation is the quotient $\tau_n/q_n$ dropping to zero or its relative difference to $\tau_{n-1}/q_{n-1}$ becoming less than $10^{-4}$. These values were determined through experimentation. We decided to use an evenly spaced mesh for simplicity, as the computation of any $g(\tau_0)$ requires the computation of $g$ for many other values in the interval $[0, \tau_0]$.

Theoretically, $g(\tau)$ is non-decreasing, so that $g'(\tau) = \lambda(\sigma)$ is positive; but using experimental data yielded non-monotonical $g(\tau)$ profiles. We analysed six data sets from [12], and for four of those we obtained good results working around the lack of monotonicity by
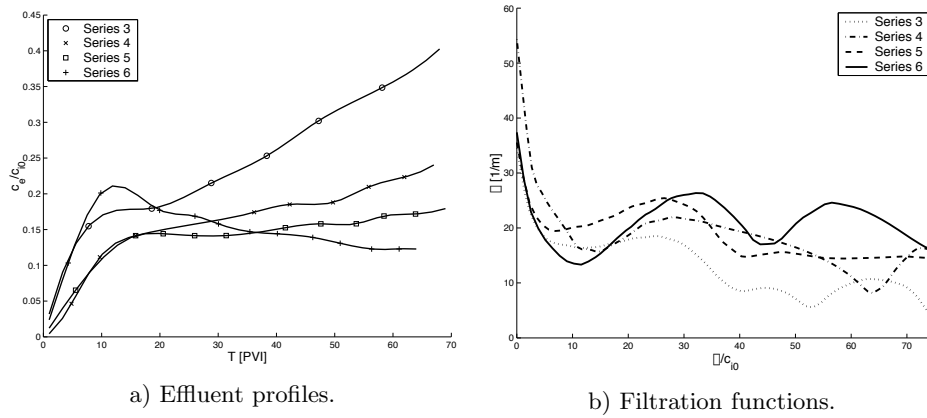
a) Effluent profiles.

b) Filtration functions.

FIGURE 5.1. Shown as markers on the left, the data series for which we solved the inverse problem. The solid lines are the effluent concentrations calculated on the basis of the recovered filtration functions; the latter are shown on the right.

removing the decreasing intervals of the function, forcing it to stay constant at the maximum at the left of each such interval. Finally, we use $g(\tau)$ to evaluate $\lambda(\sigma)$ as given in (3.11).

Figure 5.1 shows our primary results: on Figure 5.1a, we show as markers the data points of the series 3 through 6 we obtained from [12]. For each of these data series, $\lambda(\sigma)$ was recovered; these are shown in Figure 5.1b. Finally, the effluent profiles found by solving the direct problem using the recovered $\lambda(\sigma)$ are shown as solid lines in 5.1a. The oscillations in the filtration functions are due to insufficient smoothness of the data sets. Smoother data would yield smoother filtration profiles.

5.2. **The effect of extrapolating for missing data.** Experimental data for the break-through concentration $c_e(1)$ is usually unavailable. These difficulties arise from diffusive the small value of $\sigma$ at breakthrough and from difusive effects. The value of $c_e(1)$ is a key scaling factor for the whole procedure, and its sensitivity relative to the value of $c_e(1)$ was tested in the second experiment. We repeated the previous runs using the same data preprocessing, but setting $c_e(1) = c_e(T_0)$ now, where $T_0$ is the actual PVI value of the first data point available where $c_e > 0$. The resulting data series are identical to those used previously except near $T = 1$. As it can be seen in Figure 5.2, the filtration functions recovered from these series are very similar to the previous ones, except for very low $\sigma$ values, i.e. the changes at $c_e(1)$ affected mostly the neighbourhood of $\lambda(0)$, as expected. For higher $\sigma$ values, there is little change in the effluent profiles produced using the filtration functions recovered through the funcional equation, despite the unavailability of the $c_e(1)$ datum. One can set the value of $c_e(1)$ quite arbitrarily without affecting the shape of the filtration function for higher $\sigma$ values.

5.3. **The impact of data smoothing.** In our next experiment, we used a fine mesh and linear interpolation before smoothing the data with the cubic splines, so as to preserve its sharp edges. The results, analogous to those of the first experiment, are shown in Figure 5.3. Once again, the direct problem reproduces the input data with great accuracy, and the filtration functions show the same oscillating nature, however more edgy. The oscilations
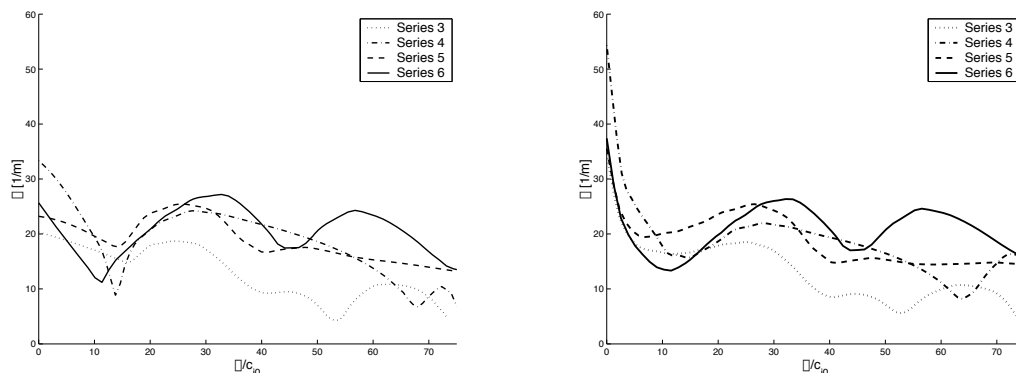
a) Filtration functions for data with imposed $c_e(1)$.    b) Filtration functions from previous experiment.

FIGURE 5.2. On the left, the filtration coefficients obtained from the series where the value of $c_e(1)$ was imposed. The figure on the right is the same as 5.1b. Comparing both Figures, notice the difference for low $\sigma$, and the similarity of the profiles as $\sigma$ increases.

are therefore due to higher values of the lower order derivatives of the curves implied by the data series.
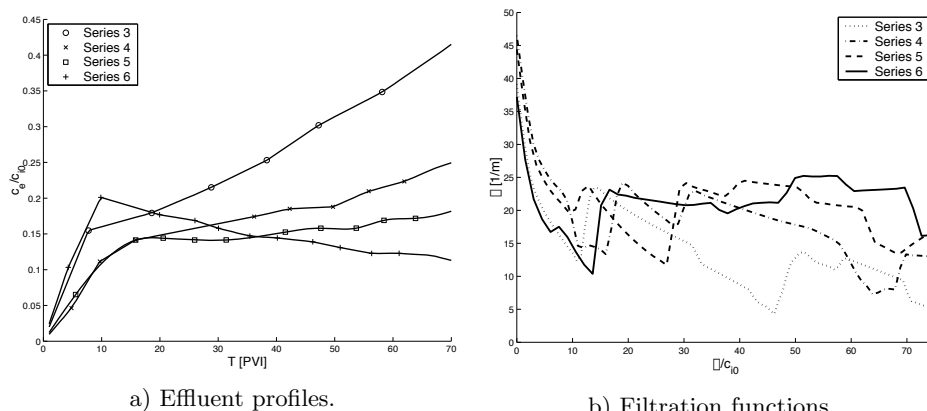


a) Effluent profiles.                    b) Filtration functions.

FIGURE 5.3. Third experiment. Same as in Figure 5.1, but using linear interpolation when preprocessing the effluent profile data.

5.4. **The effect of data preprocessing.** This model for the filtration function recovers the data series exactly, accounting for all irregularities in the data. However, because of experimental error, it is common practice in engineering to preprocess the data and replace it with smooth curves that do not necessarily pass through the experimental points; usually some sort of least square approximation is used. Figure 5.4a shows smooth profiles obtained from the data points using a preprocessing method described in a forthcoming work; applying the algorithm described here to these profiles yielded the extremely smooth filtration functions shown in 5.4b, which look much more reasonable than those in 5.2b. We calculated the effluent concentrations using these filtrations and plotted them over the input data on Figure 5.4a, with which they coincide visually.
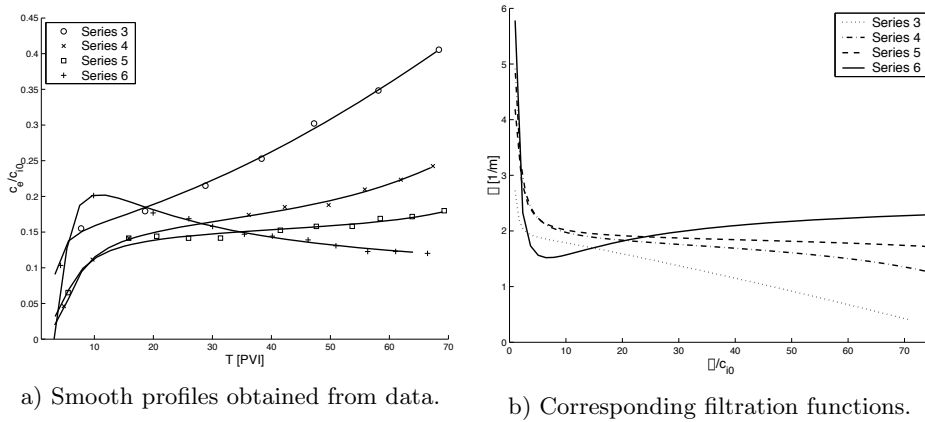
a) Smooth profiles obtained from data.

b) Corresponding filtration functions.

FIGURE 5.4. Exact recovery obtained using the functional equation over smooth aproximation of the actual data.

## 6. CONCLUSION

The method described here reduces the inverse problem of recovering the empirical filtration coefficient from measurements of effluent concentration to solving a functional equation. Taking smooth experimental data functions we obtain a nice inverse problem, with a unique solution. We presented a stable numerical method which, short of numerical errors, provides perfect matching between prescribed and predicted data, both for synthetic and for experimental data. As long as the effluent concentration is sufficiently smaller than the injected concentration, the method is not impaired by the lack of the breakthrough data on which the calculations rely, and maintains consistency with the raw data through different filtering approaches at the preprocessing stage. The quality of the recovered filtration functions depends heavily on the type of preprocessing done, and good preprocessing methods should be further investigated.

## REFERENCES

[1] A. C. Alvarez. *Inverse problems for deep bed filtration in porous media*. PhD thesis, IMPA. Brasil, 2005.

[2] P. G. Bedrikovetsky, D. Marchesin, G. Hime, A. G. Siqueira, A. L. Serra, J. R. P. Rodriguez, A. O. Marchesin, and M. Vinicius. Inverse problem for treatment of laboratory data on injectivity impairment. In *International Symposium and Exhibition on Formation Damage Control. Society of Petroleum Engineers. SPE 86523*, 2004.

[3] P. G. Bedrikovetsky, D. Marchesin, F. Shecaira, A. L. Serra, and E. Resende. Characterization of deep bed filtration system from laboratory pressure drop measurements. *Journal of Petroleum Science and Engineering*, 64(3):167–177, 2001.

[4] P. G. Bedrikovetsky, D. Marchesin, F. S. Shecaira, A. L. Serra, A. O. Marchesin, E. Rezende, and G. Hime. Well impairment during sea/produced water flooding: treatment of laboratory data. In *SPE Latin American and Caribbean Petroleum Engineering Conference*, 2001.

[5] D. D. Bui and P. Nelson. Existence and uniqueness of an inverse problem for a hyperbolic system of lidar probing. *Inverse Problem*, 5:821–829, 1992.

[6] R. Courant and D. Hilbert. *Methods of Mathematical Physics*. John Wiley, Vol. II, 1962.

[7] M. S. Espedal, A. Fasano, and A. Mikelic. Filtration in porous media and industrial application. In *Lecture Notes in Mathematics, 1734*. Springer-Verlag, 1981.

[8] J. P. Herzig, D. M. Leclerc, and P. Le. Goff. Flow of suspensions through porous media-application to deep filtration. *Industrial and Engineering Chemistry*, 65(5):8–35, 1970.

[9] F. John. *Partial Differential Equations*. Springer, 1982.

[10] M. Kuczma. *Functional Equations in a Single Variable*. Polish Scientific Publishers,Warszawa, 1968.

[11] M. Kuczma, B. Choczewski, and G. Roman. *Iterative Functional Equations*. Cambridge University Press, 1990.

[12] F. Kuhnen, K. Barmettler, S. Bhattacharjee, M. Elimelech, and R. Kretzschmar. Transport of iron oxide colloids in packed quartz sand media: Monolayer and multilayer deposition. *Journal of Colloid and Interface Science*, 231:32–41, 2000.

[13] D. J. Logan. *Transport Modeling in Hydrogeochemical Systems*. Springer-Verlag, 2001.

[14] S. Pang and M. M. Sharma. A model for predicting injectivity decline in water injection wells. In *69th Annual Technical Conference and Exhibition. New Orleans. Society of Petroleum Engineers. SPE 28489*, 1994.

[15] A. G. Ramm. On stable numerical differentiation. *Math. Comp.*, 70:1131–1153, 2001.

[16] C. H. Reinsch. Smoothing by spline functions. *Numerische Mathematik*, 10:177–183, 1967.

[17] K. I. Wennberg and M. M. Sharma. Determination of the filtration coefficient and the transition time for water injection wells. In *Society of Petroleum Engineers. SPE 38181*, 1997.